Numerical evaluation of strain transfer model for steel-reinforced optical fiber cable embedded in a cylindrical concrete beam with two void inclusions

Mira Kabbara[1,2*], *Xavier* Chapeleau[1,2], *Qinghua* Zhang[1,2], and *Frédéric* Bourquin[3]

[1]COSYS-SII, Université Gustave Eiffel, 44340 Bouguenais, France
[2]I4S, Inria, 35042 Rennes, France
[3] Université Gustave Eiffel, 77420 Champs-sur-Marne, France

Abstract. In distributed optical fiber sensors, strain transfer is usually described through a simplified one-dimensional equation, derived from continuum mechanics. This equation, in which a parameter known as the strain-lag parameter takes into account the cable's geometric and mechanical characteristics, establishes a relationship between the measured longitudinal strain profile within the optical fiber and the real strain profile occurring in the host material. In the case of steel-reinforced optical fiber cables, appreciated for their resistance to breakage during on-site instrumentation, a notable discrepancy between the measured and actual strain profiles is revealed especially in the presence of a strain gradient, indicating that the ability to transfer strain from the host material to the optical fiber is restrained using this type of cable. This paper assesses numerically the strain transfer model for steel-reinforced optical fiber sensors in the presence of a strain gradient generated by two void inclusions in a concrete beam. The good accuracy of the strain transfer model is observed by the comparison with a 3D finite element simulation. However, the result points out the critical necessity of precisely determining the strain-lag parameter.

1 Introduction

In recent years, distributed optical fiber sensors, particularly those whose technology is based on Rayleigh backscattering, have become increasingly popular for Structural Health Monitoring due to their ability to provide real-time, high-resolution measurements along the entire fiber length [1-3]. These sensors are especially effective for detecting unlocalized and invisible cracks. Optical fibers, typically made of several protective coatings to prevent breakage, provide a blurred measurement of the real strain profile in the monitored structure. This phenomenon, referred to as strain transfer, can lead to misinterpretation of strain profiles, influenced by the type of optical fiber cable used. Efforts have been made to model this phenomenon, usually with a one-dimensional second-order differential equation that incorporates the cable's properties through a parameter known as the strain-lag parameter

* Corresponding author: mira.kabbara@univ-eiffel.fr

[4-6]. Indeed, this parameter depend on the mechanical and geometric properties of the cable, such as the radius, Young's modulus and Poisson's ratio of each layer and stiffness coefficient between consecutive layers. Achieving full strain transfer is particularly challenging for optical fiber sensors with multiple coating layers and steel reinforcement, especially in the presence of strain gradients. Despite this, steel-reinforced cables are beneficial for harsh environments and complex installations [7]. Most existing research studies simplify strain profiles as linear or bilinear functions as in [8]. This paper, however, addresses a more complex scenario with an arbitrary strain gradient, applying the strain transfer model proposed in [9] to steel-reinforced optical fiber sensors. First, a 3D finite element simulation on a cylindrical concrete beam with two void inclusions is conducted, and the resulting strain profiles are used to validate the model. Then, a study was done on the impact of erroneous beta values on the model's validity, as this parameter is influenced by the cable's properties, which are often unknown and can lead to potential inaccuracies.

2 Strain transfer model applied to a steel-reinforced optical fiber sensor

For this study, a representative model of a common steel-reinforced cable on the market is chosen and it is supposed to embedded into a concrete structure of length L. The steel-reinforced cable is composed of a glass fiber with a diameter of approximately 10 µm, surrounded by an optical cladding. This optical cladding typically has a diameter of125 µm. To increase the cable's durability, three protective layers are added: a steel coating that is further enclosed by two polymer layers. To simplify, the core and cladding are considered as a single layer, referred to as the core. About that, the system in question consists of a four-layered model as the one described in [9] and for which a formula is given for the calculation a strain lag parameter, $\boldsymbol{\beta}$. To remind, the strain profiles, $\boldsymbol{\varepsilon_f}$ and $\boldsymbol{\varepsilon_m}$,in the optical fiber and in the host material respectively, are linked by:.

$$\begin{cases} \varepsilon''_f(z) - \beta^2 \varepsilon_f(z) = -\beta^2 \varepsilon_m(z) \\ \varepsilon_f(0) = \varepsilon_0;\ \varepsilon_f(L) = \varepsilon_L \end{cases} \quad (1)$$

Where z represents the coordinate along the length of the cable.

3 Validation approach for the proposed model: computing the solution of the strain transfer model using Finite difference method

The strain-lag parameter, determined through the expression provided in [9], along with the longitudinal strain outputs obtained at discrete points from a 3D Finite Element simulation on the host material level (used as input of equation (1)), are employed to solve the second-order differential equation in (1) using the Finite Difference method, as elaborated in the subsequent discussion.

The space discretization into n+1 points, labelled as z_i, is outlined as follows:

$$z_i = ih \; where \; h = \frac{L}{n} \; and \; 0 \le i \le n \quad (2)$$

The Finite Difference method is employed to approximate the second derivative of ε_f in equation (1):

$$\epsilon''_f(z_i) = \frac{\varepsilon_f(z_{i+1}) - 2\varepsilon_f(z_i) + \varepsilon_f(z_{i-1})}{h^2} \; with \; 0 \le i \le n-1 \quad (3)$$

Substituting this approximation into (1) yields:

$$a\ \varepsilon_f(z_{i+1}) + b\ \varepsilon_f(z_i) + a\varepsilon_f(z_{i-1}) = -\beta^2 \varepsilon_m(z_i) \quad (4)$$

$$where \; a = \frac{1}{h^2} \; and \; b = -\frac{2}{h^2} - \beta^2$$

The equation (4) can be expressed as a linear system represented as follows:

$$AX = b \quad (5)$$

where

$$A = \begin{pmatrix} 1 & 0 & 0 & 0 & 0 & \dots & \dots & 0 \\ a & b & a & 0 & 0 & \dots & \dots & 0 \\ 0 & a & b & a & 0 & \dots & \dots & 0 \\ 0 & 0 & a & b & a & 0 & \dots & 0 \\ \vdots & \vdots & \ddots & \ddots & \ddots & \ddots & \ddots & \vdots \\ 0 & 0 & \dots & 0 & a & b & a & 0 \\ 0 & 0 & \dots & \dots & 0 & a & b & a \\ 0 & 0 & \dots & \dots & 0 & 0 & 0 & 1 \end{pmatrix},$$

and

$$X = \begin{pmatrix} \varepsilon_f(z_0) \\ \varepsilon_f(z_1) \\ \varepsilon_f(z_2) \\ \vdots \\ \varepsilon_f(z_{n-1}) \\ \varepsilon_f(z_n) \end{pmatrix} \quad and \; b = \begin{pmatrix} \varepsilon_0 \\ -\beta^2\varepsilon_m(z_1) \\ -\beta^2\varepsilon_m(z_2) \\ \vdots \\ -\beta^2\varepsilon_m(z_{n-1}) \\ \varepsilon_L \end{pmatrix}$$

Solving the linear system in equation (5) yields ε_f at discrete points, representing the calculated strain profile in the optical fiber. A comparison is then made between the results of the 1D model and 3D simulation outcomes at the optical fiber level. Subsequently, a criterion for error is defined to assess the 1D model's accuracy. The described validation approach is detailed in Fig.1.

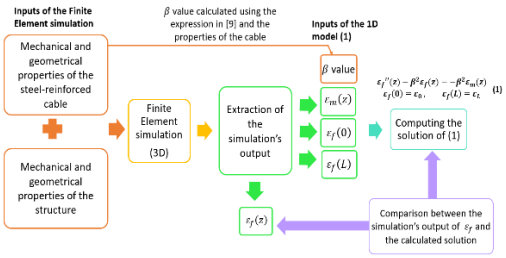

Fig. 1. Diagram representing the inputs and outputs of the 1D model.

4 Description of the three-dimensional simulation: a cylindrical beam including two inclusions with a steel-reinforced cable embedded at the center

A simulation is performed on a cylindrical concrete beam measuring 600 mm in length and 100 mm in radius, incorporating two void inclusions, as illustrated in Fig. 2. These void inclusions are characterized as annular regions resembling rings, defined by their geometric parameters. Each inclusion features an outer radius of 7 cm and an inner radius of 5 cm. The presence of these void inclusions can significantly affect the mechanical behavior of the concrete beam, influencing stress distribution within the structure and effectively creating a strain gradient. The beam is subjected to a tensile force of 125 kN. A 1-meter steel-reinforced optical fiber cable, with a radius of 1 mm, comprising an optical fiber and two polymer coatings encasing a steel coating, is embedded at the center of the structure. Based on the cable properties provided in Table 1 and the strain lag parameter expression given in [9], the strain lag parameter is found to be $\beta = 8.5\ m^{-1}$.

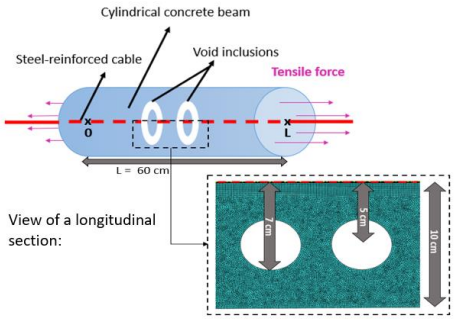

Fig.2. Cylindrical concrete beam with two inclusions and steel-reinforced cable in the center.

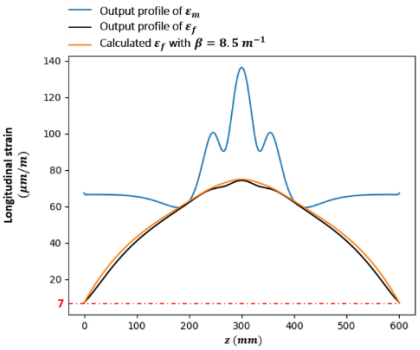

Fig.3. Simulation's outputs of the strain vs the 1D model's solution using appropriate boundary conditions (ε_0=ε_L=7 µm/m) and $\beta = 8.5\ m^{-1}$

Table 1. Geometric and mechanical properties of the optical fiber cable's components.

Layer	Radius (mm)	Young Modulus (GPa)	Poisson 's ratio	Interfacial stiffness coefficient (Mpa/mm)
Optical fiber	0.06	70	0.3	10
Coating 1	0.12	1	0.4	10
Coating 2	0.77	200	0.3	10
Coating 3	1	4	0.4	10

5 Strain transfer model validity with appropriate boundary conditions and β value

The results obtained from the earlier discussed numerical simulation serve to validate the model proposed in (1). Within Fig.3, the longitudinal strain profiles of both the optical fiber ε_f and the host material ε_m of the 3D finite element simulation are represented by the black and blue curves, respectively. It is crucial to emphasize the smoothing effect of the optical cable on deformation measurements, as highlighted by the significant difference between the two extracted profiles. Employing the ε_m profile at discrete points alongside the previously determined beta value $\beta = 8.5$ m^{-1} as inputs, the differential equation (1) is solved using the Finite Difference method, as previously discussed. Boundary conditions are derived from the simulation's output of longitudinal strain at the optical fiber level, specifically denoted as ε_0=ε_L=7 µm/m. The resulting solution, which portrays the computed longitudinal strain in the optical fiber, is illustrated by the orange curve in Fig.3. A comparison is then made between this profile and the longitudinal strain output of the 3D model in the optical fiber. The error between the simulation's output and the calculated strain profile in the core remains below 3 µm/m. This strong agreement between the outputs of the 3D and 1D models at the core level points out the model's accuracy for the case studied.

6 Assessment of the strain transfer model validity under varied strain-lag parameter's values

While the outcomes appear suitable, it's crucial to examine how the value of the beta parameter might affect the reliability of the model since this parameter is linked to the mechanical and geometric characteristics of the sensor, which are often unknown consequently the beta value. Therefore, it becomes necessary to investigate the influence of using an erroneous beta value in the mechanical transfer model and to determine the acceptable margin of error required to achieve accurate results using the 1D model. In this context, equation (1) is solved for various beta values, utilizing the strain profile at the concrete beam level obtained from the numerical simulation and ensuring appropriate boundary conditions are applied (ε_0=ε_L=7 µm/m). Subsequently, for each value of beta, the error between the calculated profile and the simulation's strain profile in the optical fiber is assessed at each point. As evaluation criteria, we consider that an error of less than 4 µm/m at a point implies that the model yields acceptable results. The selected beta value is deemed suitable also if the extent of invalid areas does not surpass 100 mm from either end and provides valid results within the z-interval [100,500]. Fig.4 where the model is considered valid, i.e., according the chosen criteria, for a range of β value. It is demonstrated that the values of β between 7.4

and 9 m^{-1}, delimited as the green zone in Fig.4, provide validity of the model throughout at least two-thirds of the entire cable's length. However, values outside this interval yield inaccurate results, particularly in the center of the cable and at both ends.

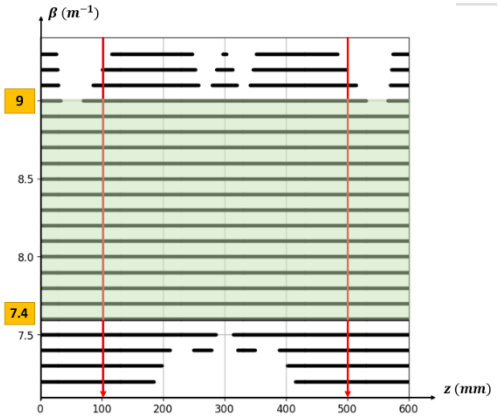

Fig.4. Zones of validity of the 1D model with several values of β

7 Conclusion

In conclusion, this paper evaluated through a numerical simulation the mechanical strain transfer model for steel-reinforced cable in the presence of a strain gradient generated by two inclusions in a cylindrical concrete beam. The results demonstrated the cable's smoothing effect on strain measurements. Additionally, the one-dimensional strain transfer model is validated, with errors remaining within acceptable limits, provided the strain-lag parameter was accurately estimated. However, accurately characterizing the cable remains a significant challenge due to insufficient information from manufacturers. Even minor errors in the strain-lag parameter, β, led to erroneous results.

Furthermore, a gap in the literature persists regarding the inverse problem of the strain transfer model, which focuses primarily on the direct problem, assuming known strain profiles within the host material. However, in on-site applications, this profile is often unavailable, requiring more in-depth studies.

References

1. Pierre Ferdinand, “The Evolution of Optical Fiber Sensors Technologies During the 35 Last Years and Their Applications in Structure Health Monitoring”, 7th European Workshop on Structural Health Monitoring July 8-11, 2014. La Cité, Nantes, France.

2. Barrias A, Casas JR, Villalba S. A Review of Distributed Optical Fiber Sensors for Civil Engineering Applications, Sensors (Basel), May 2016

3. Brian J. Soller, Dawn K. Gifford, Matthew S. Wolfe, and Mark E. Froggatt,” High-resolution optical frequency domain reflectometry for characterization of components and assemblies,” Opt. Express 13, 666-674 (2005)

4. Farhad Ansari and Yuan Libo, “Mechanics of Bond and Interface Shear Transfer in Optical Fiber Sensors,” Journal of Engineering Mechanics, vol. 124, no. 4, pp. 385-394, 1998.

5. Huaping Wang and Zhi Zhou, “Advances of strain transfer analysis of optical fiber sensors,” Pacific Science Review, vol. 7677, pp.8–18, Sep. 2014.

6. Antoine Bassil, Distributed Fiber Optics Sensing for Crack Monitoring of Concrete Structures, PhD thesis, Université de Nantes, Nov. 2019.

7. Arianna Piccolo et al., “Mechanical Properties of Optical Fiber Strain Sensing Cables under γ-Ray Irradiation and Large Strain Influence,” Sensors (Basel, Switzerland), vol.20, no. 3, p. 696, Jan. 2020

8. Xing Zheng, Bin Shi, Cheng-Cheng Zhang, Yijie Sun, Lei Zhang, Heming Han, “Strain transfer mechanism in surface-bonded distributed fiber-optics sensors subjected to linear strain gradients: Theoretical modeling and experimental validation”, Measurement, Volume 179, 2021

9. Xavier Chapeleau and Antoine Bassil, “A General Solution to Determine Strain Profile in the Core of Distributed Fiber Optic Sensors under Any Arbitrary Strain Fields,” Sensors, vol. 21, no. 16, pp. 1–33, Jan. 2021.